Nanolithographic Write, Read, and Erase via Reversible Nanotemplated Nanostructure Electrodeposition on Alkanethiol-Modified Au(111) in an Aqueous Solution

Kyoungja Seo and Eric Borguet*

Department of Chemistry, Temple University, Philadelphia, Pennsylvania 19122

Received September 12, 2005. In Final Form: December 12, 2005

A write, read, and erase nanolithographic method, combining in situ electrodeposition of metal nanostructures with atomic force microscopy (AFM) nanoshaving of a 1-hexadecanethiol (HDT) self-assembled monolayer (SAM) on Au(111) in an aqueous solution, is reported. The AFM tip defines the local positioning of nanotemplates via the irreversible removal of HDT molecules. Nanotemplates with lateral dimensions as narrow as 25 nm are created. The electroactive nanotemplates determine the size, shape, and position of the metal nanostructures. The potential applied to the substrate controls the amount of metal deposited and the kinetics of the deposition. Metal nanostructures can be reversibly and repeatedly electrodeposited and stripped out of the nanotemplates by applying appropriate potentials.

The creation of metal nanostructures of predetermined shape is of interest for the fabrication of electrical and optical components of miniature electronic devices.[1,2] Metallic nanosize wires, dots, and tubes have been prepared using electrodeposition or electroless deposition combined with various methods such as membrane[3,4] and self-organized templates,[5−10] microcontact printing,[11] edge lithography,[12] step-edge method,[13−15] electron beam nanolithography,[16,17] and scanning probe microscopy (SPM) nanolithography.[8,18−22] However, previous metal nanostructure nanofabrication processes have employed irreversible processes, that is, only the writing and reading steps. To date, no erase capability has been demonstrated.

Electrochemical deposition is a simple method to prepare metal structures on conducting substrates. Electrochemical fabrication of metal nanostructures has been reported using SPM-based lithography, typically by tip-induced electrochemical deposition of metal ions transferred by the scanning tunneling microscopy (STM) or atomic force microscopy (AFM) tip to the surface.[18−21] A potential, externally applied to the substrate, can control the electrochemical reaction rate at the interface. In particular, the amount of deposit and the kinetics of the metal deposition onto the surface can be controlled. Because the electrochemical process is sensitive to the surface properties, in situ local deposition of metal can be made selective by tuning the surface characteristics. For example, the electrochemical deposition of metal should occur predominantly in a hydrophilic region rather than in a hydrophobic area of the surface.[23−25]

A number of SPM lithographic methods have been reported. Patterns can be made using an AFM tip to mechanically scratch away an organic thin film (nanoshaving).[26−29] Nanografting has been used for nanostructure fabrication, for example, thiol-tethered nanoparticles and biomaterials in the nanoshaved patterns.[28−35] Direct nanoscale patterning methodologies, such as dip-pen nanolithography,[20] the nanopen "reader and writer" method,[30] and conductive AFM nanolithography,[36] have also constructed various organic and metal nanoparticle architectures. Recently, the galvanic deposition of metal after static plowing lithography of a polymer resist was used to prepare patterns of metallic nanostructures.[37] However, these were irreversible processes and accomplished with ex situ procedures.

While a combination of nanolithography and electrodeposition for metal nanostructure formation might appear to be a natural solution, a number of problems have become apparent. In situ

* Corresponding author. E-mail: eborguet@temple.edu.

(1) Fasol, G.; Runge, K. *Appl. Phys. Lett.* **1997**, *70*, 2467.
(2) Favier, F.; Walter, E. C.; Zach, M. P.; Benter, T.; Penner, R. M. *Science* **2001**, *293*, 2227.
(3) Brumlik, C. J.; Martin, C. R. *J. Am. Chem. Soc.* **1991**, *113*, 3174.
(4) Foss, C. A.; Hornyak, G. L.; Stockert, J. A.; Martin, C. R. *J. Phys. Chem.* **1994**, *98*, 2963.
(5) Attard, G. S.; Bartlett, P. N.; Coleman, N. R. B.; Elliott, J. M.; Owen, J. R.; Wang, J. H. *Science* **1997**, *278*, 838.
(6) Bartlett, P. N.; Gollas, B.; Guerin, S.; Marwan, J. *Phys. Chem. Chem. Phys.* **2002**, *4*, 3835.
(7) Elliott, J. M.; Attard, G. S.; Bartlett, P. N.; Coleman, N. R. B.; Merckel, D. A. S.; Owen, J. R. *Chem. Mater.* **1999**, *11*, 3602.
(8) Hoeppener, S.; Maoz, R.; Sagiv, J. *Nano Lett.* **2003**, *3*, 761.
(9) Liu, S. T.; Maoz, R.; Schmid, G.; Sagiv, J. *Nano Lett.* **2002**, *2*, 1055.
(10) Xu, D. W.; Graugnard, E.; King, J. S.; Zhong, L. W.; Summers, C. J. *Nano Lett.* **2004**, *4*, 2223.
(11) Azzaroni, O.; Schilardi, P. L.; Salvarezza, R. C. *Electrochim. Acta* **2003**, *48*, 3107.
(12) Yang, H.; Love, J. C.; Arias, F.; Whitesides, G. M. *Chem. Mater.* **2002**, *14*, 1385.
(13) Li, Q. G.; Olson, J. B.; Penner, R. M. *Chem. Mater.* **2004**, *16*, 3402.
(14) Walter, E. C.; Zach, M. P.; Favier, F.; Murray, B. J.; Inazu, K.; Hemminger, J. C.; Penner, R. M. *ChemPhysChem* **2003**, *4*, 131.
(15) Zoval, J. V.; Lee, J.; Gorer, S.; Penner, R. M. *J. Phys. Chem. B* **1998**, *102*, 1166.
(16) Sondag-Huethorst, J. A. M.; Fokkink, L. G. J. *Langmuir* **1995**, *11*, 4823.
(17) King, G. M.; Schurmann, G.; Branton, D.; Golovchenko, J. A. *Nano Lett.* **2005**, *5*, 1157.
(18) Berenz, P.; Xiao, X. Y.; Baltruschat, H. *J. Phys. Chem. B* **2002**, *106*, 3673.
(19) Li, Y.; Maynor, B. W.; Liu, J. *J. Am. Chem. Soc.* **2001**, *123*, 2105.
(20) Porter, L. A.; Choi, H. C.; Schmeltzer, J. M.; Ribbe, A. E.; Elliott, L. C. C.; Buriak, J. M. *Nano Lett.* **2002**, *2*, 1369.
(21) Zamborini, F. P.; Crooks, R. M. *J. Am. Chem. Soc.* **1998**, *120*, 9700.
(22) Zhang, H.; Jin, R. C.; Mirkin, C. A. *Nano Lett.* **2004**, *4*, 1493.
(23) Li, Q. G.; Zheng, J. W.; Liu, Z. F. *Langmuir* **2003**, *19*, 166.
(24) He, H. X.; Zhang, H.; Li, Q. G.; Zhu, T.; Li, S. F. Y.; Liu, Z. F. *Langmuir* **2000**, *16*, 3846.
(25) Zhu, T.; Fu, X. Y.; Mu, T.; Wang, J.; Liu, Z. F. *Langmuir* **1999**, *15*, 5197.
(26) Amro, N. A.; Xu, S.; Liu, G. Y. *Langmuir* **2000**, *16*, 3006.
(27) Xiao, X. D.; Liu, G. Y.; Charych, D. H.; Salmeron, M. *Langmuir* **1995**, *11*, 1600.
(28) Xu, S.; Liu, G. Y. *Langmuir* **1997**, *13*, 127.
(29) Xu, S.; Miller, S.; Laibinis, P. E.; Liu, G. Y. *Langmuir* **1999**, *15*, 7244.
(30) Garno, J. C.; Yang, Y. Y.; Amro, N. A.; Cruchon-Dupeyrat, S.; Chen, S. W.; Liu, G. Y. *Nano Lett.* **2003**, *3*, 389.
(31) Guiducci, C.; Stagni, C.; Zuccheri, G.; Bogliolo, A.; Benini, L.; Samori, B.; Ricco, B. *Biosens. Bioelectron.* **2004**, *19*, 781.
(32) Liu, G. Y.; Xu, S.; Qian, Y. L. *Acc. Chem. Res.* **2000**, *33*, 457.
(33) Liu, J. F.; Cruchon-Dupeyrat, S.; Garno, J. C.; Frommer, J.; Liu, G. Y. *Nano Lett.* **2002**, *2*, 937.
(34) Liu, M. Z.; Amro, N. A.; Chow, C. S.; Liu, G. Y. *Nano Lett.* **2002**, *2*, 863.
(35) Nuraje, N.; Banerjee, I. A.; MacCuspie, R. I.; Yu, L. T.; Matsui, H. *J. Am. Chem. Soc.* **2004**, *126*, 8088.
(36) Fresco, Z. M.; Suez, I.; Backer, S. A.; Frechet, J. M. J. *J. Am. Chem. Soc.* **2004**, *126*, 8374.
(37) Porter, L. A.; Ribbe, A. E.; Buriak, J. M. *Nano Lett.* **2003**, *3*, 1043.

10.1021/la052489l CCC: $33.50
Published on Web 01/19/2006

Scheme 1. In Situ Fabrication of Metal Nanostructures through a Combination of AFM Nanoshaving and Electrodeposition

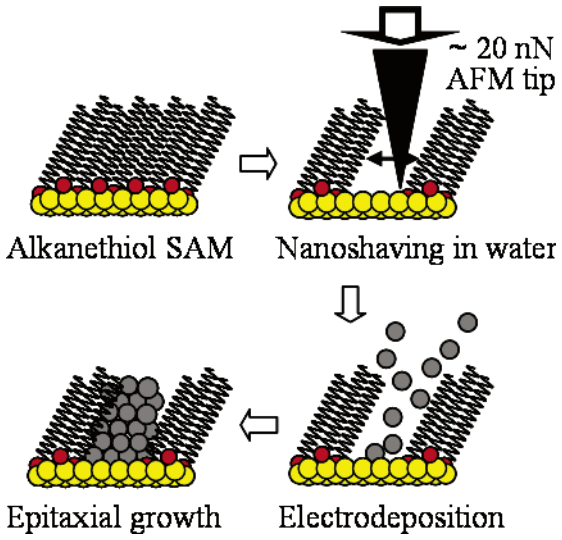

STM studies of local electrodeposition of metal showed that tip charging can electrostatically impede the diffusion of metal ions to the area under the tip.[38] In other studies, AFM tip scanning was used to change the local reactivity of the surface underneath the tip, enhancing the local deposition of polypyrrole on highly oriented pyrolitic graphite[39] and that of Cu on a Cu single crystal[40,41] and enhancing the local dissolution of Al[42] and p-GaAs-(100).[43] AFM tip-induced surface reactions must be controlled to achieve in situ preparation of metal nanostructures. For example, Gewirth et al. reported the nanoscale electrodeposition of metal in nanopatterned alkanethiol-modified Au(111).[41] Although the interaction between the tip and sample enhanced Cu deposition on the surface, Cu did not deposit uniformly in the area scanned, but only deposited at the edges of the scanned area as well as in defects of the alkanethiol self-assembled monolayer (SAM). The authors suggested physical and electrostatic inhibition, by the tip, of the diffusion of Cu ions to the area under the tip, even on a bare Au(111) surface.[41]

We report a write, read, and erase nanolithography via reversible, nanotemplated nanostructure electrodeposition on the Au(111) surface. We demonstrate the reversible, single-pot, nanolithographic patterning of metal nanostructures in an insulating template, in a manner that allows for writing (metal deposition), reading (imaging), and erasing (metal dissolution). The introduction of reversibility should improve the flexibility and usefulness of nanolithography. We have combined AFM nanoshaving and electrodeposition (Scheme 1) and accomplished in situ, reversible fabrication of metal nanostructures on a nanotemplated surface in a single solution. This procedure combines the advantages of local high-resolution positioning of nanofeatures with control of the deposition process provided by electrochemistry. The potential controls the amount of deposit and the kinetics of metal deposition. The AFM tip defines the local positioning of nanofeatures. Selective deposition of Ag is successfully, reproducibly, and reversibly obtained in the nanotemplate defined by nanoshaving.

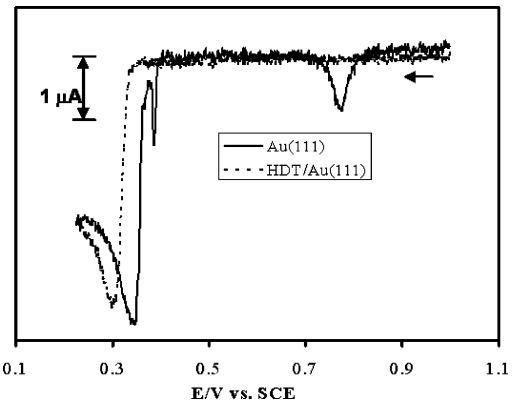

Figure 1. Linear sweep voltammograms for Ag electrodeposition in an HDT SAM/Au(111) and a bare Au(111) electrode in 0.1 M $HClO_4$ containing 1 mM $AgClO_4$ at 10 mV s^{-1}.

1-Hexadecanethiol (HDT) SAMs were prepared by immersing an Au(111) single-crystal disk (Mateck GmbH, Germany) for over 15 h into a solution of 1 mM HDT (Aldrich) in ethanol. Au(111) was chemically cleaned by hot piranha solution (1:3 H_2O_2 (J. T. Baker, CMOS) and H_2SO_4 (J. T. Baker, CMOS)) (**Caution! Piranha solution is a very strong oxidant and is extremely dangerous to work with; gloves, goggles, and a face shield should be worn**), followed by hydrogen flame annealing before use. Cyclic voltammetry of 1 mM $K_3Fe(CN)_6$ (Alfa Aesar, ACS grade) in a 0.1 M HNO_3 (Fisher Scientific Co.) solution was employed to evaluate HDT SAMs on Au(111).[44−46] AFM (Picoscan, Molecular Imaging) imaging was performed in contact mode with about 0.5 nN of applied force, at least an order of magnitude less than the force applied for nanoshaving. Potential control and voltammetry employed a bipotentiostat (Picostat, Molecular Imaging). The electrochemical cell was composed of a Au(111) working electrode and Pt wires as the reference and counter electrodes. All potentials are quoted versus the saturated calomel electrode (SCE). AFM nanoshaving was performed with an oxide-sharpened silicon nitride tip (Veeco, ORC8) with a force constant of 0.1 N/m in a 0.1 M $HClO_4$ (Fisher Scientific Co., trace metal grade) solution containing 1 mM $AgClO_4$ (Aldrich). All AFM images reported here were obtained at open circuit potential (OCP).

The linear sweep voltammogram of bare Au(111) in 0.1 M $HClO_4$ containing 1 mM $AgClO_4$ clearly shows Ag underpotential deposition (UPD) peaks around 0.8 and 0.4 V and a feature indicating the onset of the bulk deposition around 0.38 V, the Ag/Ag^+ Nernst potential, at a Ag^+ concentration of 1 mM (Figure 1).[47] A highly ordered HDT SAM/Au(111) apparently suppresses UPD and retards Ag bulk deposition, as the current does not rise until about 40 mV negative of the Nernst potential (Figure 1). This overpotential of Ag bulk deposition on the HDT SAM/Au(111) is close to the value reported for 1-octadecanthiol SAM.[47] An HDT SAM presumably prevents Ag^+ ions from penetrating the underlying substrate. The voltammogram suggests that, at low overpotential, Ag can be electrochemically deposited only onto bare Au, with no electrodeposition occurring on the HDT SAM passivated surface.

AFM nanoshaving to make a nanoscale bare area of Au in an HDT SAM/Au(111), that is, a nanotemplate, was successfully performed in a 0.1 M $HClO_4$ solution containing 1 mM $AgClO_4$.

(38) Batina, N.; Kolb, D. M.; Nichols, R. J. *Langmuir* **1992**, *8*, 2572.
(39) Cai, X. W.; Gao, J. S.; Xie, Z. X.; Xie, Y.; Tian, Z. Q.; Mao, B. W. *Langmuir* **1998**, *14*, 2508.
(40) Lagraff, J. R.; Gewirth, A. A. *J. Phys. Chem.* **1994**, *98*, 11246.
(41) Lagraff, J. R.; Gewirth, A. A. *J. Phys. Chem.* **1995**, *99*, 10009.
(42) Chen, L. L.; Guay, D. *J. Electrochem. Soc.* **1994**, *141*, L43.
(43) Koinuma, M.; Uosaki, K. *Surf. Sci.* **1996**, *358*, 565.
(44) Chidsey, C. E. D.; Loiacono, D. N. *Langmuir* **1990**, *6*, 682.
(45) Finklea, H. O.; Avery, S.; Lynch, M.; Furtsch, T. *Langmuir* **1987**, *3*, 409.
(46) Porter, M. D.; Bright, T. B.; Allara, D. L.; Chidsey, C. E. D. *J. Am. Chem. Soc.* **1987**, *109*, 3559.
(47) Hagenstrom, H.; Esplandiu, M. J.; Kolb, D. M. *Langmuir* **2001**, *17*, 839.

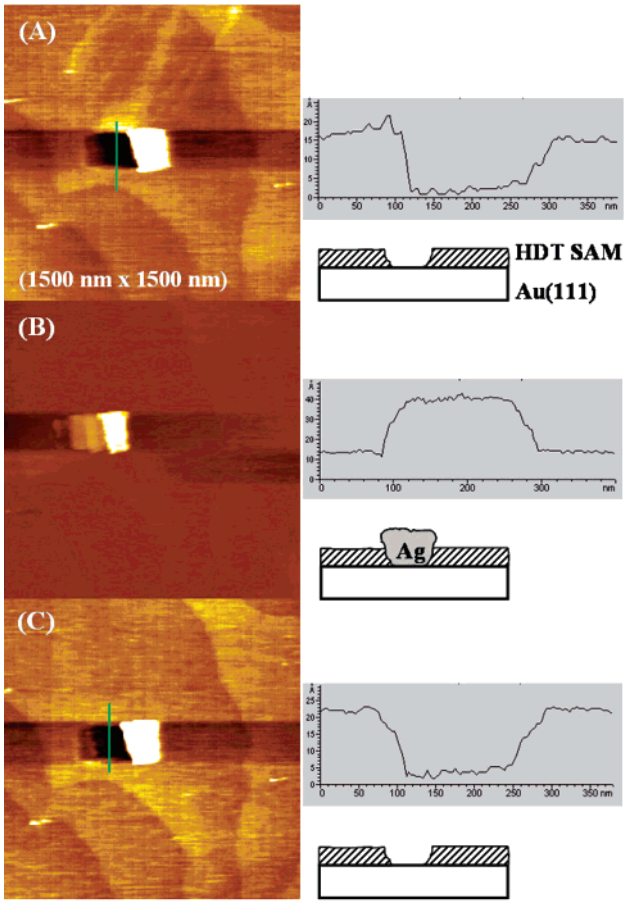

Figure 2. AFM images of Ag nanostructures electrodeposited in the nanotemplate created in an HDT SAM/Au(111). Images were obtained at OCP in 0.1 M $HClO_4$ containing 1 mM $AgClO_4$ (A) after nanoshaving, (B) after applying 0.36 V for 1 min, and (C) after applying 0.56 V for 1 min.

The tip scanned the selected area three times with a force of about 20 nN at OCP, creating a nanotemplate of about 150 × 150 nm^2 (Figure 2A). In an aqueous solution, the displaced molecules can remain weakly attached to the surface and the edge of the nanotemplate because of their poor solubility in water.[48] However, the displaced molecules do not appear to come back into the pattern on the time scale of metal electrodeposition but remain piled up at the right boundary of the nanotemplate. The depth of the nanotemplate, ∼15 Å in Figure 2A, in the cross-section of the AFM image is smaller than the physical thickness of an HDT SAM (∼20 Å[45,46]). This is probably due to the adsorbed molecules remaining inside the pattern or the SAM molecules outside the pattern being compressed by the tip scanning.[49] In control experiments, the nanotemplates were stable at OCP and over the potential range of 0.3 to −0.1 V for as long as 40 min with no noticeable change in shape and depth.

To construct the Ag nanostructure in the nanotemplate, the tip was retracted by 0.2 μm during the application of potentials. This procedure can prevent artifacts caused, for example, by the tip interfering with the diffusion of Ag ions and/or driving chemical reactions as a result of the frictional force between the tip and the substrate.[39−43] These phenomena are poorly understood. The retraction of the tip simplifies the process so that the electrodeposition is controlled, in principle, only by the applied potential in the nanotemplate.

A Ag nanostructure (Figure 2B) was deposited to a height of about 2.6 nm above the surface in the nanotemplate after 1 min at 20 mV negative of the Nernst potential, 0.36 V. At this potential, Ag electrodeposition takes place only on the exposed Au, that is, the nanotemplate. AFM images revealed that Ag^+ did not perturb highly ordered regions of the SAM. The height of the nanostructure was determined to increase with longer deposition time.

Reversible patterning, that is, the ability to read, write, and erase, is highly desirable. To demonstrate that the nanoelectrodeposition is reversible, the nanotemplate was imaged after holding at 0.56 V for 1 min. Clearly, the surface has returned to what appears to be the initial state (Figure 2C). The cross-section analysis of the pattern reveals that the Ag nanostructure is removed at 0.56 V. Evidence for desorption of the SAM was not observed. Ag electrodeposition and stripping were successfully repeated in the nanotemplate multiple times with apparently no change in surface morphology.

A useful nanodeposition process should be characterized by precise control of the location of the deposition. The AFM images and cross-section analysis (Figure 2) indicate only deposition and stripping of Ag nanostructure in the nanotemplate, as opposed to reactions involving the Ag deposition onto the top of the SAM and/or the desorption of adsorbed HDT molecules. The highly ordered HDT SAM used in this study can prevent the bulk electrodeposition and underpotential deposition of Ag at moderate overpotentials (≤ 40 mV) (Figure 1). Ag electrodeposition does not appear to take place in areas outside the template (Figure S1, Supporting Information). Thus it appears that, at a low overpotential, the HDT SAM limits deposition to the nanoshaved area. At high overpotentials (> 40 mV), however, bulk deposition of Ag can occur in the defects, and it grows up in a mushroom shape to cover the SAM.[47,50] Thus, we restricted our investigations to moderate potentials from low underpotentials (e.g., 0.46 V) to low overpotentials (e.g., 0.34 V). When combined with nanoshaving, the electrochemical process can be selectively limited to the interface between the exposed gold of the nanotemplate and an electrolyte solution.

A complete HDT SAM protects the surface against Ag^+ penetration. Defects in the HDT SAM do not allow penetration of Ag^+ under the present condition, as shown in voltammograms (Figure 1) and AFM images (Figure S1, Supporting Information). On the other hand, defects in the incomplete SAM could allow penetration of ions to the surface.[51] This would provide nucleation sites for both bulk Ag electrodeposition and underpotential deposition. For example, Ag deposition takes place in defects in an incomplete SAM (Figure S2, Supporting Information). In the present case, when a highly ordered SAM is employed, Ag underpotential deposition takes place exclusively in the nanoshaved template.

Successful dissolution of Ag nanostructures at a low underpotential (e.g., 0.56 V) suggests there is no formation of a complex between Ag and HDT. Place exchange of thiol molecules from the Au substrate to the deposited Ag could take place.[21] The fact that Ag nanostructures can be grown suggest that either thiol place exchange between Au and Ag surfaces is not occurring or that it does not influence the Ag growth. In aqueous solution, it appears that thiol diffusion is very slow, as revealed by the stability of the nanoshaved patterns. If thiol place exchange occurs, dissolution of the deposited Ag could be retarded or inhibited

(48) Liu, G. Y.; Salmeron, M. B. *Langmuir* **1994**, *10*, 367.
(49) Patterson, J. E.; Dlott, D. D. *J. Phys. Chem. B* **2005**, *109*, 5045.
(50) Sondag-Huethorst, J. A. M.; van Helleputte, H. R. J.; Fokkink, L. G. J. *Appl. Phys. Lett.* **1994**, *64*, 285.
(51) Oyamatsu, D.; Kuwabata, S.; Yoneyama, H. *J. Electroanal. Chem.* **1999**, *473*, 59.

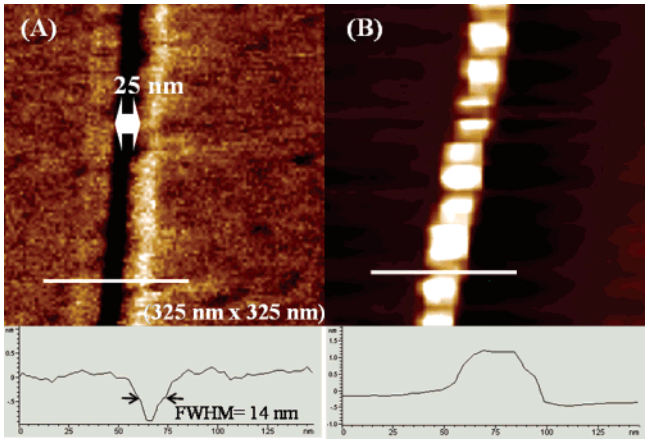

Figure 3. AFM images (deflection) of an HDT SAM/Au(111) for Ag electrodeposition (A) after nanoshaving and (B) after applying 0.36 V for 1 min. Images were obtained at OCP in 0.1 M $HClO_4$ containing 1 mM $AgClO_4$.

by the formation of a SAM on the Ag nanostructure.[21,52] However, the cross-sectional analysis in Figure 2C reveals that a Ag nanostructure in the template clearly dissolved in 1 min.

We have demonstrated the fabrication of sub-50-nm-scale Ag nanostructures via a combination of nanoshaving and electrodeposition, as illustrated by the creation of a 25 nm wide nanotemplate (Figure 3A) in which a Ag nanowire (Figure 3B) is formed by applying 0.36 V for 1 min. This pattern reveals the capability of this technique to design nanostructured surfaces, such as nanowiring.

The nanotemplate constrains the growth of the Ag nanostructure to the vertical dimension. Generally, the growth rate of the metal deposit in the plane of the surface is faster than that normal to the surface.[38,53] However, the nanotemplate provides a perimeter barrier to limit the lateral growth of Ag nanostructure and leads to vertical growth. Therefore, the height of the Ag nanostructure in the nanotemplate can be controlled by the applied potential value and the deposition time.

The growth rate of Ag nanostructures in the nanotemplate was examined as a function of the potential applied to the substrate (Figure 4). Ag electrodeposition in the nanotemplate was not observed until the application of overpotential. At 20 mV negative of the Nernst potential (Figure S3B, Supporting Information), the pattern was filled with a 2.3 nm high Ag deposit in 1 min (Figure 4). The growth rate of Ag nanostructures was remarkably accelerated with the utilization of a more negative overpotential. At 40 mV negative of the Nernst potential (Figure S3C, Supporting Information), the rate of Ag bulk deposition was significantly faster; 3.3 nm of Ag nanostructure was created within 1 s (Figure 4). A longer exposure time ($\geq$1 min) led to continuous growth of Ag nanostructures beyond the nanotemplate.

The results described in this paper demonstrate reversible patterning using the combination of AFM nanoshaving and metal electrodeposition/dissolution. In addition to the interest and novelty associated with this demonstration, there are a number

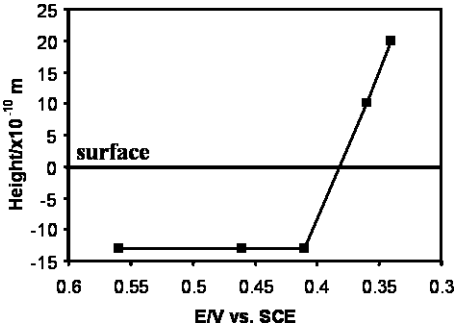

Figure 4. Plot of the height of the nanotemplated region as a function of applied potential. Electrode potential was held at 0.56, 0.46, 0.41, and 0.36 V for 1 min and 0.34 V for 1 s.

of applications. First, patterned metal nanostructures in insulating SAMs can act as templates for further modification; for example, the metal nanostructures can be useful substrates for the attachment of biomolecules.[54] Second, the reversibility of Ag nanowire patterning can provide a pattern with alternating optical reflectivity on the nanometer scale, where the surface can reversibly provide two different optical properties under potential control.[55]

In summary, we have shown the reversible, "single-pot" construction of Ag nanostructures in an HDT SAM/Au(111) by combing in situ electrodeposition and AFM nanoshaving in an aqueous solution. The nanotemplate in the HDT SAM/Au(111) was stable with the applied potential over the time of electrodeposition. Retracting the tip during deposition and stripping avoids effects such as the enhancements or suppression of metal deposition and dissolution. An externally applied potential allows for successful, reproducible, and selective deposition and the stripping of metal nanostructures in the nanotemplates. Our results demonstrate that electrodeposition can be combined with nanoshaving to develop a nanolithographic technique that allows for writing (metal deposition), reading (imaging), and erasing (metal dissolution). The in situ, local electrodeposition of metal can be used to fabricate complex nanostructures in an aqueous solution. The reversible nature of the procedure extends the capabilities of nanolithography.

Acknowledgment. This work was supported by the NSF (CHE 0456965). K.S. acknowledges the support of the Postdoctoral Fellowship Program of the Korea Science & Engineering Foundation (KOSEF).

Supporting Information Available: AFM images of the effect of externally applied potential on Ag electrodeposition in the nanotemplate of an HDT SAM/Au(111) (S3), an HDT SAM/Au(111) before and after Ag electrodeposition (S1), and a poor, incomplete HDT SAM/Au(111) after Ag electrodeposition (S2). This material is available free of charge via the Internet at http://pubs.acs.org.

LA052489L

(52) Li, W. J.; Virtanen, J. A.; Penner, R. M. *Langmuir* **1995**, *11*, 4361.
(53) Kolb, D. M.; Ullmann, R.; Ziegler, J. C. *Electrochim. Acta* **1998**, *43*, 2751.
(54) Rosi, N. L.; Mirkin, C. A. *Chem. Rev.* **2005**, *105*, 1547.
(55) Nicewarner-Pena, S. R.; Carado, A. J.; Shale, K. E.; Keating, C. D. *J. Phys. Chem. B* **2003**, *107*, 7360.